

## The HPM-100-40 Hybrid Detector

The bh HPM-100 module combines a Hamamatsu R10467-40 GaAsP hybrid PMT tube with the preamplifier and the generators for the PMT operating voltages in one compact housing. The principle of the hybrid PMT in combination with the GaAsP cathode of the R10467-40 yields excellent timing resolution, a clean TCSPC instrument response function, high detection quantum efficiency, and extremely low afterpulsing probability. The virtual absence of afterpulsing results in a substantially increased dynamic range for fluorescence decay recordings. FCS curves down to 100 ns correlation time can be obtained from a single detector, without the need of cross-correlation. The HPM-100 module is operated via the bh DCC-100 detector controller of the bh TCSPC systems.

### Principle

The basic principle of a hybrid PMT is shown in Fig. 1. The photoelectrons emitted by a photocathode are accelerated by a strong electrical field and injected directly into a silicon avalanche diode [4, 8].

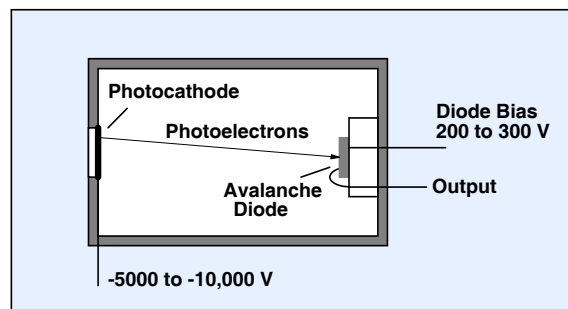


Fig. 1: Principle of a hybrid PMT

When an accelerated photoelectron hits the avalanche diode it generates a large number of electron-hole pairs in the silicon. These carriers are further amplified by the linear gain of the avalanche diode. The principle of the hybrid PMT has a number of advantages over other detector principles.

An obvious advantage of the hybrid PMT is that a large part of the gain is obtained in a single step. Hybrid PMTs therefore deliver single-photon pulses with a narrow amplitude distribution. The devices can thus be used to distinguish between one, two, or even more photons detected simultaneously [8]. In TCSPC applications the low amplitude fluctuation virtually eliminates the influence of the CFD circuitry on the timing jitter.

More important for TCSPC, the high acceleration voltage between the photocathode and the APD results in low transit time spread [4]. With an acceleration voltage of 8 kV the transit-time spread of the electron time-of-flight is only 50 ps [4, 5]. Moreover, the TCSPC instrument response of a hybrid PMP is very clean, without significant tails, bumps, or secondary peaks.

Compared to a conventional PMT, the hybrid PMT has also an advantage in terms of counting efficiency. In a conventional PMT, a fraction of the photoelectrons is lost on the first dynode of the

electron multiplication system [1]. Instead of being multiplied electrons may also get absorbed or reflected. There are no such losses in the hybrid PMT: A photoelectron accelerated to an energy of 8 keV is almost certain to generate a signal in the avalanche diode. With a high-efficiency GaAsP cathode a hybrid photomultiplier reaches the efficiency of a single-photon APD (SPAD), but with a cathode area several orders of magnitude larger.

The perhaps most significant advantage of the hybrid PMT has been recognised only recently: The hybrid PMT is virtually free of afterpulsing [2]. Afterpulsing is the major source of counting background in high-repetition-rate TCSPC applications, and a known problem in fluorescence correlation measurements. Background has a detrimental effect on the accuracy of fluorescence lifetime determination [6]. Afterpulsing in FCS results in a false peak at correlation times shorter than a few  $\mu\text{s}$ . So far, the afterpulsing peak could only be suppressed by splitting the light and recording cross-correlation between two detectors.

The absence of afterpulsing in a hybrid PMT is inherent to its design principle. In conventional PMTs afterpulsing is caused by ionisation of residual gas molecules by the electron cloud in the dynode system. In single-photon avalanche photodiodes afterpulsing results from trapped carriers of the previous avalanche breakdown. Both effects do not exist in the hybrid PMT: Ionisation is negligible because only single electrons are travelling in the vacuum, and there is no avalanche breakdown in the APD.

On the downside, there are also a few disadvantages of the hybrid PMT. The extremely high cathode voltage is difficult to handle. It can be a problem especially in clinical biomedical applications. The APD reverse voltage must be very stable, and be correctly adjusted. The most significant problem is the low gain of the hybrid PMTs. Earlier devices reached a gain on the order of only  $10^4$ . At a gain this low, the single-photon pulse amplitude is in the  $\mu\text{V}$  range. Therefore electronic noise from the termination resistor and from the preamplifier impaired the time resolution of single photon detection. Until recently, hybrid PMTs were therefore not routinely used for TCSPC experiments. The situation changed with the introduction of the R10467 hybrid PMTs of Hamamatsu [5]. The devices reach a total gain on the order of  $10^5$ . The single-photon pulse amplitude is on the order of several  $100 \mu\text{V}$ , the pulse width about 800 ps. A high bandwidth, low-noise preamplifier is able to amplify the pulses into an amplitude range where they are detected by the constant-fraction discriminator of a bh TCSPC module. Initial tests have shown the superior performance of the R10467 compared to previously existing detectors [2]. However, in practice RF noise pickup from the environment, noise from the high voltage power supplies, and low-frequency currents flowing through ground loops make the bare R10467 tube difficult to use in TCSPC experiments.

## **The bh HPM-100 Hybrid Detector Module**

To make the R10467 applicable to standard TCSPC experiments bh have integrated the R10467 tube, the power supply for the cathode voltage, the power supply for the APD voltage, and the preamplifier in a compact, carefully shielded detector module. The device is shown in Fig. 2.

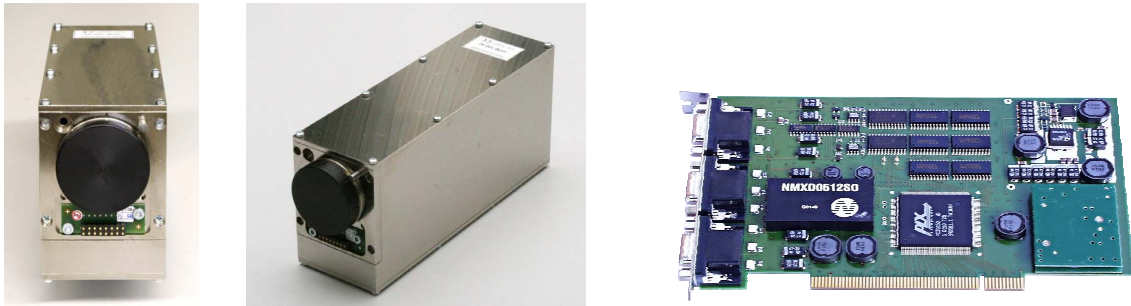


Fig. 2: bh HPM-100 hybrid PMT module. The module contains the Hamamatsu R10467 hybrid PMT tube, the generators for the cathode voltage and the APD reverse voltage, and the preamplifier. The module is operated via the DCC-100 card of the bh TCSPC systems (right)

The housing has separate compartments for the voltage generators, the R10467 tube, and the preamplifier. These are shielded and decoupled against each other and the environment. The complete module is operated via the bh DCC-100 detector controller card. The DCC-100 provides for power supply, control of the APD reverse voltage, and overload shutdown. One DCC-100 card can control two HPM-100 hybrid PMT modules.

### Instrument response function

The instrument response function of an HPM-100-40 with an R10467-40 tube is shown in Fig. 3.

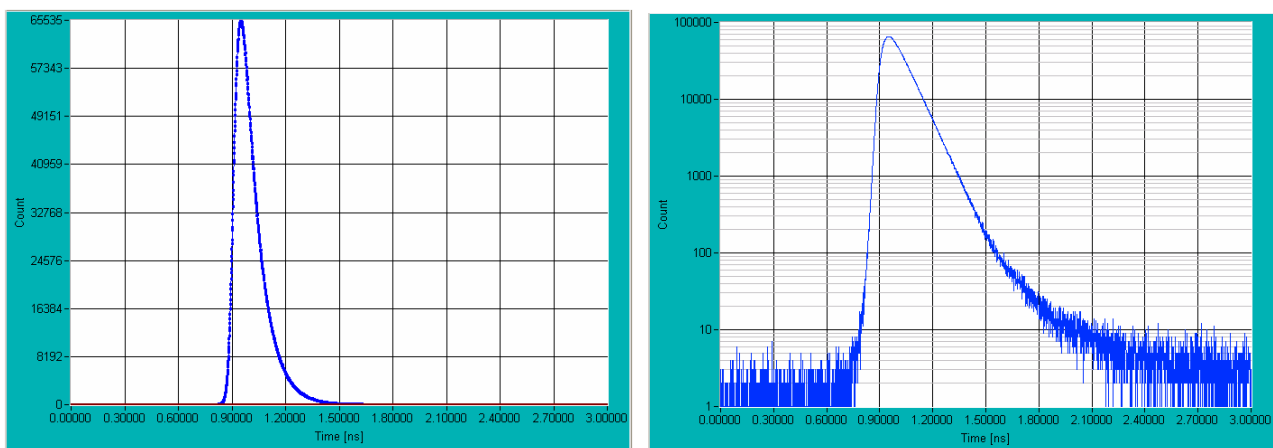


Fig. 3: Instrument response function of the HPM-100-40. Left: linear scale. Right: Logarithmic scale. BDL-445 SMC picosecond diode laser, bh SPC-830 TCSPC module.

The recorded instrument response function (IRF) width is 130 ps. Corrected for the laser pulse width of 60 ps the IRF width is about 120 ps. The response function is remarkably clean, as can be seen in the logarithmic plot on the right. It should be noted that the transit time spread and thus the IRF width of the R10467-40 is dominated by the internal time constants of its GaAsP cathode. The R10467-06 tube (with a conventional bialkali cathode) is faster, with an IRF width of about 50 ps.

### Afterpulsing

The afterpulsing is characterised best by the autocorrelation function of the photons of a continuous light signal detected at a known count rate [1, 2]. Fig. 4 compares the autocorrelation function of an HPM-100-40 at 10 kHz count rate with that obtained by a Hamamatsu H5773-1 photosensor

module. The autocorrelation for the HPM is flat down to the dead time of the SPC-830 module used. Comparable performance has been achieved so far only for NbN superconducting detectors. These detectors have active areas with  $\mu\text{m}$  extensions and need to be operated in a liquid-He cryostat [9].

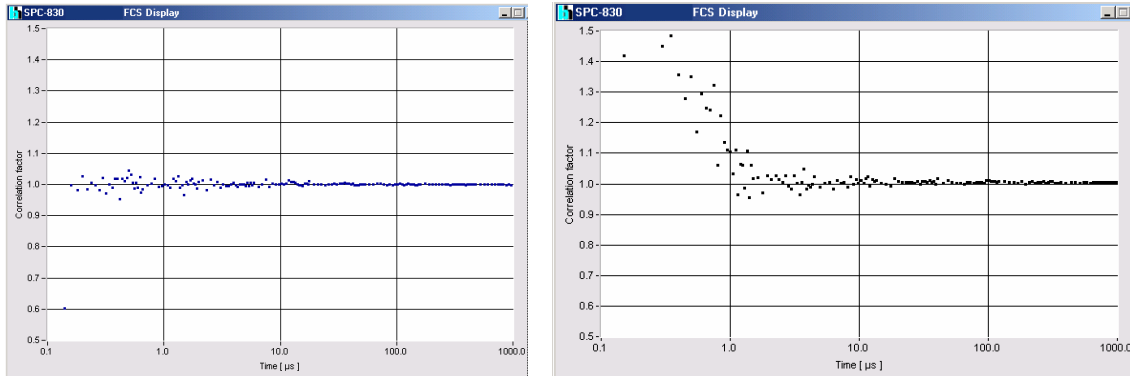


Fig. 4: Autocorrelation function of a continuous light signal of 10 kHz count rate. Left: HPM-100-40. Right: H5773-1. The autocorrelation function measured with the HPM is flat down to 125 ns, indicating that no afterpulses are detected.

Fig. 5 shows an FCS curve measured for a solution of fluorescein in water. The data were recorded by an HPM-100-40 connected to the bh DCS-120 confocal scanning FLIM system [3]. Because there is no afterpulsing peak diffusion and triplet times are obtained by autocorrelation of the photons detected in a single detector.

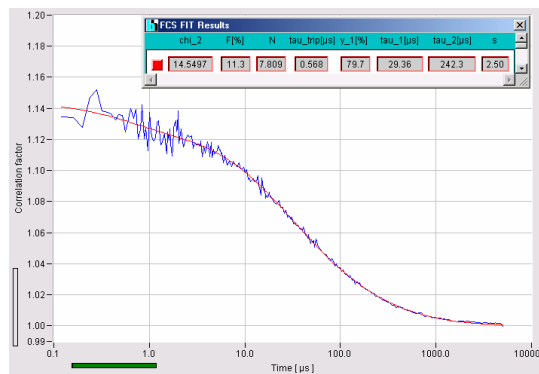


Fig. 5: Fluorescence correlation function of fluorescein molecules in water. Recorded with HPM-100-40, connected to bh DCS-120 confocal scanning FLIM system

The low afterpulsing results in a significantly improved dynamic range of fluorescence decay measurements. An example is shown in Fig. 6. It shows the fluorescence decay of fluorescein recorded at a laser repetition rate of 20 MHz. The signal was detected by a HPM-100-40 (left) and a H5773-1 photosensor module (right). Both detectors have approximately the same dark count rates.

For the HPM-100, the dark count rate is the only source of background. Because the dark count rate is only a few 100 counts per second an extraordinarily high dynamic range is obtained. For the H5773-1 the background is dominated by afterpulsing. The background is substantially higher, and the dynamic range is far smaller than for the HPM-100.

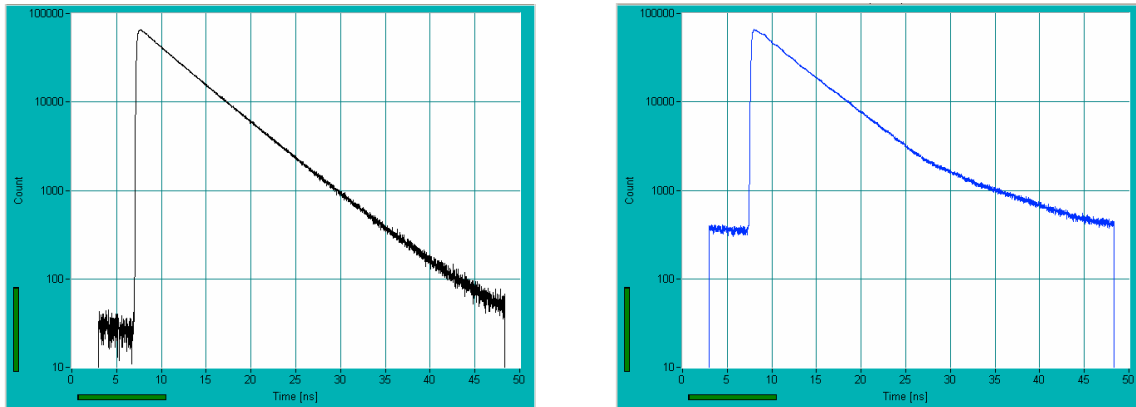


Fig. 6: Fluorescence decay curves for fluorescein recorded at a laser repetition rate of 20 MHz. Left: HPM-100-40. Right: H5773-01

## Sensitivity

We had no possibility to verify the detection quantum efficiency of the R10467-40 quantitatively. The curve of cathode quantum efficiency versus wavelength shown in Fig. 7, left, was therefore copied from the specifications of Hamamatsu [5]. What we could verify, however, is that the detection efficiency surpasses the efficiency for the Hamamatsu H7422P-40. The H7422P-40 has the same cathode type but uses a conventional PMT design. Until now, the H7422P-40 was the ultimate in sensitivity for visible-range PMTs. The HPM reaches at least the same efficiency, but at a far better time resolution and without any afterpulsing.

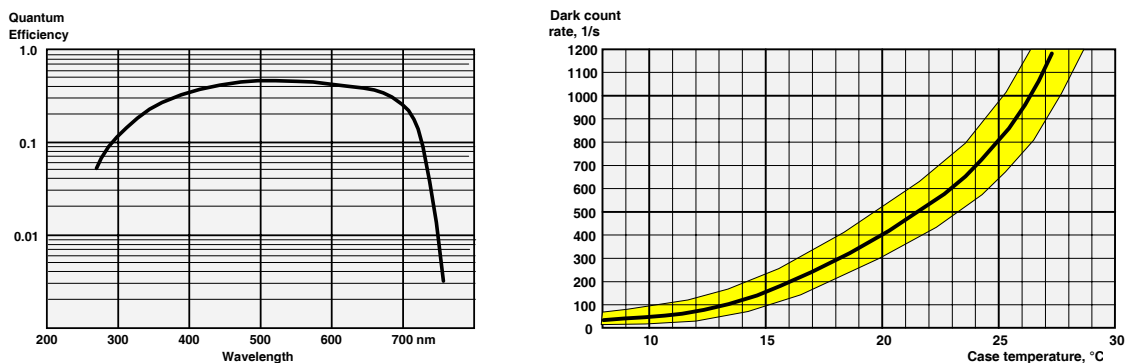


Fig. 7: Left: Detection quantum efficiency according to Hamamatsu specification. Right: Dark count rate. Black curve average of 4 detectors. Yellow area: Range of variation for 7 detectors, measured over several days.

For low-level light detection the limiting parameter is often not only the efficiency but also the dark count rate. Typical curves of the dark count rate versus temperature are shown in Fig. 7, right. The values we found are a bit lower than the numbers in the Hamamatsu test sheets, and significantly lower than the numbers given in [7]. The reasons are not clear. It should be noted that low dark count rates are only obtained if (a) the reverse voltage of the avalanche diode is selected below the breakdown level and (b) the tube has been kept in darkness for several hours after any exposure to daylight.

## The advantage of large active area

In most applications it is difficult or even impossible to concentrate the light to be detected on an extremely small area. A typical case is multiphoton microscopy. Multiphoton microscopy is used to obtain images from image planes deep in a sample. The fluorescence photons from these layers are scattered on the way out of the sample and emerge from a large area of the sample surface. Although these photons can be transferred to a detector by ‘non-descanned detection’ they cannot be concentrated on an area smaller than a few mm in diameter [1, 2].

A similar situation can exist even in a confocal microscope. Confocal detection uses a pinhole in a plane conjugate with the image plane in the sample [3]. One would expect that the light from the pinhole is easy to focus on a small detector, such as a single-photon avalanche diode (SPAD). Unfortunately, in practice this is often not the case. Normally scan heads of laser scanning microscopes have additional magnification built in so that the physical pinhole size is on the order of millimeters. Demagnifying the pinhole to the size of a SPAD by a single lens can be impossible. This is especially the case when larger pinholes, on the order of tens of Airy Units, are used.

An example is shown in Fig. 8. Both lifetime images were recorded at a pinhole size of 3 Airy Units. Data recorded with the HPM-100 are shown left, data recorded with an id-100-50 SPAD right. Despite of the fact that the quantum efficiencies of the detectors do not differ substantially the image recorded with the HPM contains about twice the number of photons as the image recorded with the SPAD.

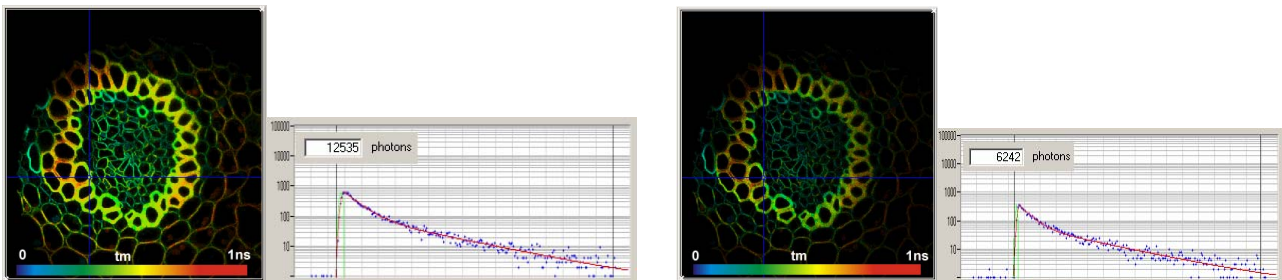


Fig. 8: Fluorescence lifetime images recorded with an HPM-100 (left) and with an id-100-50 SPAD (right). Images and decay functions at selected cursor position.

## Controlling the HPM-100-40

The HPM-100 is operated and controlled via the DCC-100 card of the bh TCSPC systems [2]. The DCC control panel is shown in Fig. 9.

For safety reasons, the DCC-100 comes up with all outputs disabled, see Fig. 9, left. Both the acceleration voltage and the reverse voltage of the avalanche diode (AD) are turned off. The panel is shown for one detector and for two detectors.

Once the outputs are enabled (‘Enable’ button) and the +12V operating voltage is turned on (+12V button) the internal high-voltage generator applies the 8 kV acceleration voltage to the R10467 tube and turns on the reverse voltage of the avalanche diode. The +5V and the -5V must also be turned on, they are used in the preamplifier. The AD reverse voltage is controlled via the ‘Gain’ sliders.

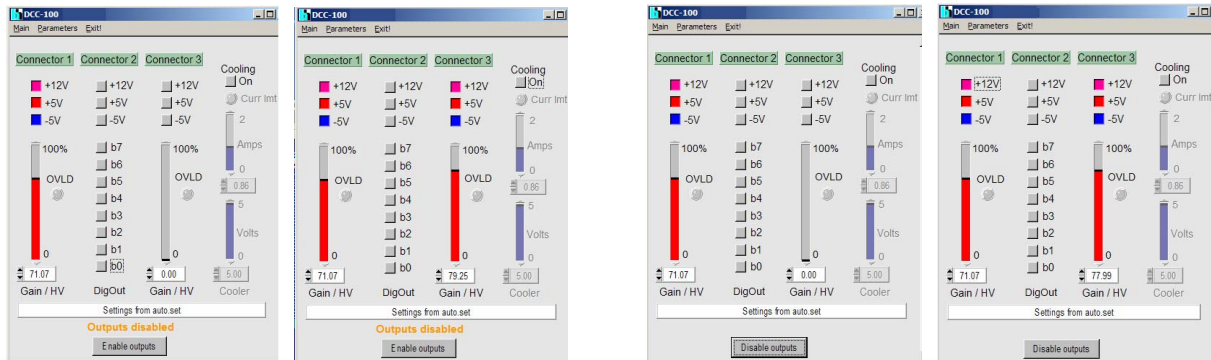


Fig. 9: DCC-100 control panel, for one detector and for two detectors. Left: After software start, the detectors are disabled. Right: Detectors enabled. The ‘Gain’ sliders control the AD voltages.

The correct selection of the operating parameters is critical to the operation of the HPM. The recommended CFD threshold of the SPC module is -30 mV. The AD reverse voltage must be selected to operate the AD close to the maximum stable gain, but not in the breakdown region.

The selection of the AD voltage is demonstrated in Fig. 10. The gain of the AD increases steeply with the voltage, see Fig. 10, left. Consequently, photon counting is obtained in a relatively narrow interval of the reverse voltage, or DCC ‘Gain’. The gain-voltage characteristics vary for different detectors. Different detectors therefore need different values of the DCC gain. The correct DCC gain can easily be found by slowly increasing the DCC gain and observing the count rate displayed by the TCSPC module. Typical curves of the count rate versus DCC Gain are shown in Fig. 10, right. At low DCC gain no counts are obtained. At a specific DCC gain the count rate rises steeply. Then it remains almost constant over an interval of 5 to 10 % of DCC Gain. Beyond this interval the count rate rises steeply. The APD is driven in the breakdown region, the APD current becomes unstable, and eventually the DCC-100 shuts the HPM-100 down. The correct operating point is in the middle of the flat part of the curve, as indicated in Fig. 10, right.

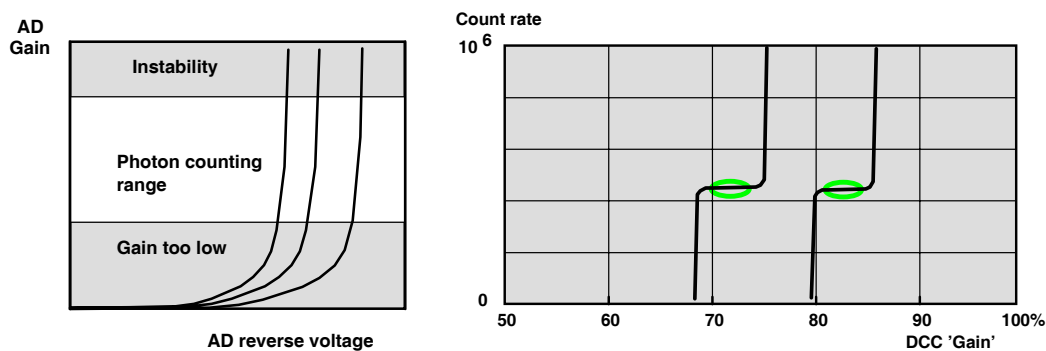


Fig. 10: Left: General dependence of the AD gain on the AD reverse voltage. Right: Dependence of the count rate on the DCC Gain for different detectors. The correct operating point is in the flat part of the curve.

If the AD current becomes too high, either because the ‘Gain’ was pulled too far up or the light intensity is too high, the DCC-100 shuts down the HPM-100. The acceleration voltage is turned off, and the APD reverse voltage is reduced down to zero. This brings the detector in a safe state. After the reason of the overload has been removed, the detector can be brought back to operation by clicking on the ‘Reset’ button. The DCC-100 panel in the overload state is shown in Fig. 11.

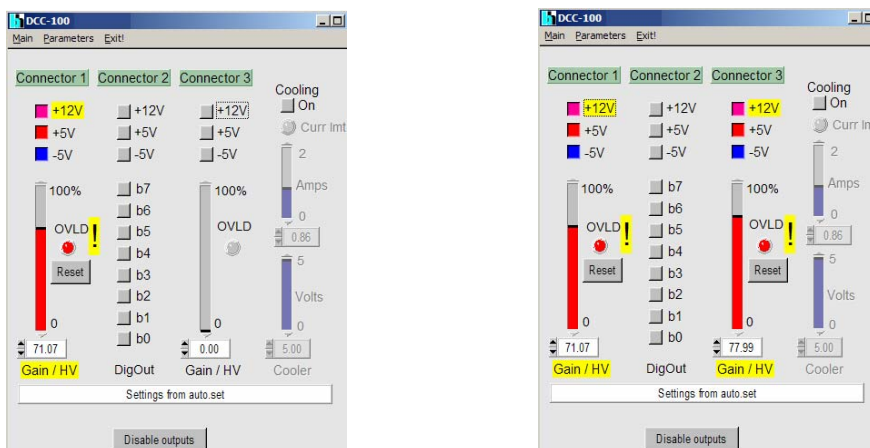


Fig. 11: DCC-100 panel after overload shutdown. Left one detector. Right: Two detectors, both detectors shut down.

## Summary

With the bh HPM-100 module, there is, for the first time, a detector that combines high speed, clean response, high efficiency, large active area, absence of afterpulsing, and ease of use. Combined with the bh TCSPC systems, it detects fluorescence decay functions with unprecedented dynamic range, has the sensitivity to efficiently acquire FCS data, and delivers FCS without the need of cross-correlation. The main area of application of the HPM-100 is time-resolved microscopy which demands for exactly the combination of parameters the HPM-100 provides. However, the HPM-100 may be used for any TCSPC experiments that require high precision, high sensitivity, and wide dynamic range.

## References

1. W. Becker, Advanced time-correlated single-photon counting techniques. Springer, Berlin, Heidelberg, New York, 2005
2. W. Becker, The bh TCSPC handbook. 3<sup>rd</sup> edition, Becker & Hickl GmbH (2008), available on [www.becker-hickl.com](http://www.becker-hickl.com)
3. Becker & Hickl GmbH, DCS-120 Confocal Scanning FLIM Systems, user handbook. [www.becker-hickl.com](http://www.becker-hickl.com)
4. A. Fukasawa, J. Haba, A. Kageyama, H. Nakazawa and M. Suyama, High Speed HPD for Photon Counting, 2006 Nuclear Science Symposium, Medical Imaging Conference, San Diego, CA (2006)
5. Hamamatsu Photonics, R10467 hybrid PMTs, data sheet.
6. M. Köllner, J. Wolfrum, How many photons are necessary for fluorescence-lifetime measurements?, Phys. Chem. Lett. **200**, 199-204 (1992)
7. X. Michalet, A. Cheng, J. Antelman, Motohiro Suyama, Katsuhiko Arisaka, Shimon Weiss, Hybrid photodetector for single-molecule spectroscopy and microscopy. Proc. SPIE 6862 (2007)
8. R.A. La Rue, K.A. Costello, G.A. Davis, J.P. Edgecumbe, V.W. Aebi, Photon Counting III-V Hybrid Photomultipliers Using Transmission Mode Photocathodes. IEEE Transactions on Electron Devices **44**, 672-678 (1997)
9. M. Stevens, R.H. Hadfield, R.E. Schwall, S.W. Nam, R.P. Mirin, Time-correlated single-photon counting with superconducting detectors. Proc. of SPIE 6372, 63720U-1 to -10